

## **Influence of Li<sup>2+</sup> Content on Formation of Apatite Layer on Surface of SiO<sub>2</sub>-CaO-K<sub>2</sub>O-P<sub>2</sub>O<sub>5</sub> Bioglass System**

**M.I. El Gohary, S.M. El-Din\*, S.M. Awad\*, Asmaa M. El-Tohamy\* and I. E. Soliman**

*Physics Department, Biophysics Branch, Faculty of Science, Al-Azhar University(Boys) and Egypt. \*Physics Department, Biophysics Branch, Faculty of Science, Al-Azhar University (Girls), Nasr City, Cairo, Egypt.*

**I**N PRESENT study, sol-gel derived glasses were prepared based on the following general formula :SiO<sub>2</sub>-CaO-P<sub>2</sub>O<sub>5</sub>-K<sub>2</sub>O and different concentrations of - Li<sub>2</sub>O (0-10 wt.%) were substituted for K<sub>2</sub>O in the studied system. The influence of these substitutions is investigated for both *in vitro* apatite formation ability and structure changes of the system. The thermal behavior of biomaterials is characterized by DSC and TGA. The precipitated crystalline phases were identified by X-ray diffraction analysis before immersion in simulated body fluid .Infrared absorption spectroscopy is performed on glass samples before and after SBF .Bioactivity results of this study suggest that formation of apatite layer depends on the concentration of Li<sub>2</sub>O which represents decrement *in vitro* bioactivity of glass . Also, it is possible to develop bioactive glass system by percentage of lithium content which controls the dissolution rate of this system to be applied *in vivo* for dentine and bone replacement.

**Keywords:** Sol-gel, Bioactive glass, *In vitro*.

Bioactive glass can adheres to bone and tissues through the formation of calcium phosphate at the interface. These materials have been used clinically as regenerative material in dental and orthopedic applications .These are considered as synthetic graft used in oral ,maxillofacial & orthopedic surgery for various indications <sup>(1)</sup>. A small change in the composition can produce a drastic effect on its behavior <sup>(2)</sup>. Glass also have an important role in drug delivery for example the biodegradation rate and physicochemical properties of drug loaded scaffolds with ciprofloxacin could be controlled by controlling the glass content and drug concentration added<sup>(3)</sup> .

However, the bioactive glasses produced from the sol-gel technique are more interested in research because of; i) Their superior bioactivity resulting from high specific surface area of these glasses yielding too many OH groups in the glass network and ii) Unlimited content of silica in the glass composition. The synthesis route play important role in modifying the glass feature. It is concluded that 52S4 is a bioactive glass if prepared by the two routes: melting or sol-gel

methods. However, this glass is more reactive when it is prepared by sol-gel method. The sol-gel route enhances the glass resorption and as a result the formation of the bone-like apatite at the glass surface<sup>(4)</sup>.

Many researchers preferred studying sol-gel derived bioactive glasses containing SiO<sub>2</sub>, CaO and P<sub>2</sub>O<sub>5</sub> as the main components of the glass composition<sup>(5)</sup>. The presence of SiO<sub>2</sub> in the composition of bioactive glasses is important because of its function as network former in the glass structure. In addition, Si-OH groups produced from the exchange process of Ca<sup>2+</sup> ions (from the glass) with H<sub>3</sub>O<sup>+</sup> (from the solution) are susceptible sites for calcium phosphate nucleation<sup>(6)</sup> meanwhile the presence of Si ions released from the glass composition into the cell culture medium can improve cell functions (such as cell proliferation and cell activity)<sup>(7)</sup>. P<sub>2</sub>O<sub>5</sub> is also used to aid nucleation of calcium phosphate phase on the glass surfaces<sup>(5)</sup>.

The system under investigation in the present work is SiO<sub>2</sub>-CaO-K<sub>2</sub>O-P<sub>2</sub>O<sub>5</sub>. Concerning the influence of lithium on bone mineral density, Clement *et al.*<sup>(8)</sup> showed that anabolic effect of lithium on bone in mice. Zamani *et al.*<sup>(9)</sup> indicated that maintenance of therapy with lithium carbonate can preserve or enhance bone density. Lithium is suggested to be incorporated to the composition of bone filler bioactive material to enhance its therapeutic properties. However it may influence surface reactivity of material with respect to apatite formation ability. The ability of material to form calcium phosphate layer on its surface determines its bioactivity<sup>(10)</sup>.

The aim of the present study is to investigate the influence of substitution of various amounts of Li<sub>2</sub>O for K<sub>2</sub>O in the system to follow the reactivity and bioactivity mechanism of dissolution/precipitation behavior in SBF solution. Other researchers used large amounts of Li<sub>2</sub>O, so that small amounts were used in this paper to know its effect on apatite formation inside the body.

## Material and Methods

### Materials

Calcium nitrate tetrahydrate Ca (NO<sub>3</sub>)<sub>2</sub>. 4H<sub>2</sub>O and lithium nitrate LiNO<sub>3</sub> were ≥ 99% Segma- Aldrich. Tetraethyl orthosilicat (TEOS), triethyl phosphate (TEP) and potassium nitrate KNO<sub>3</sub> were all ≥ 98% Buchs, Switzerland. Nitric acid 68% Merck, USA. Nitric acid was diluted to 2 M using distilled water.

### Synthesis

55% SiO<sub>2</sub>-29% CaO-6% P<sub>2</sub>O<sub>5</sub>-10% K<sub>2</sub>O system with varying amounts of Li<sub>2</sub>O was synthesized by sol-gel technique. Li<sub>2</sub>O was added to the glass composition at the expense of K<sub>2</sub>O. Table 1 represents compositional information of various glass samples prepared in present study. Initially, tetraethyl orthosilicate, distilled water, 2M nitric acid (HNO<sub>3</sub>) were successively mixed in 50 ml ethanol and the mixture was allowed to react for 90 min under continuous magnetic stirring for acid hydrolysis of TEOS. The ratio of TEOS to H<sub>2</sub>O is 1:12 and the ratio of HNO<sub>3</sub> to H<sub>2</sub>O is 1:6<sup>(5)</sup>. Then appropriate amounts of series of reagents were added in sequence. The resulted

gel formed was placed in a covered container and then the cover is removed to allow for removal of ethanol and water from the gel.

**TABLE 1. Chemical composition of various glasses containing different contents of Li<sub>2</sub>O (wt %).**

S1	55 %SiO <sub>2</sub>	10 %K <sub>2</sub> O	29 %CaO	6 %P <sub>2</sub> O <sub>5</sub>	0 %Li <sub>2</sub> O
S2	55 %SiO <sub>2</sub>	7 %K <sub>2</sub> O	29 %CaO	6 %P <sub>2</sub> O <sub>5</sub>	3 %Li <sub>2</sub> O
S3	55 %SiO <sub>2</sub>	5 %K <sub>2</sub> O	29 %CaO	6 %P <sub>2</sub> O <sub>5</sub>	5 %Li <sub>2</sub> O
S4	55 %SiO <sub>2</sub>	3 %K <sub>2</sub> O	29 %CaO	6 %P <sub>2</sub> O <sub>5</sub>	7 %Li <sub>2</sub> O
S5	55 %SiO <sub>2</sub>	0 %K <sub>2</sub> O	29 %CaO	6 %P <sub>2</sub> O <sub>5</sub>	10 %Li <sub>2</sub> O

#### *Characterization*

The as-formed gel was characterized using DSC and TGA to study the thermal properties and decomposition temperatures of various species at different temperatures. The gel specimen was placed in the specimen holder and heated from ambient temperature to 1000 °C at a heating rate of 10 °C/min with nitrogen used as purging gas. The phase analysis of the samples was examined by X-ray diffractometer, using Ni-filtered CuKα irradiation ( $\lambda=1.54 \text{ \AA}$ ) at 40 kV and 25 mA with scanning rate 0.1° in the 2θ ranging from 10 to 80° step time one second. Infrared spectra of the prepared glass samples were obtained using Fourier transform infrared spectrophotometer (FTIR). Each sample used for infrared spectroscopic analysis was prepared according to KBr technique. The changes in concentration of Ca and P ion concentration in SBF solution during 16 days of immersion of glass powders were measured by using Inductive Coupled Plasma- Optical Emission Spectroscopy (ICP-OES) technique. The morphology and microstructure of the synthesized samples were evaluated using SEM. The samples were coated with a thin layer of gold (Au) by sputtering and then the morphology of them were observed on a SEM that operated at the acceleration voltage of 30 kV.

#### *In-vitro assays in SBF*

*In vitro* assays were performed in a simulated body fluid (SBF), proposed by Kokubo *et al.*<sup>(6)</sup>. The SBF solution has a composition and concentration similar to those inorganic parts of human plasma. During soaking process, each disc with dimension (radius=0.5cm, thickness=0.2 cm) was soaked into 50 ml SBF contained in a polyethylene bottle. After being soaked, the powders were rinsed with deionized water and acetone and dried at room temperature.

## **Results and Discussion**

#### *Characterization of bioactive glass before soaking in SBF*

##### *Thermal analysis*

Thermo-gravimetric analysis (TGA) and differential scanning calorimetric (DSC), analysis curves for S1 are shown in Fig. 1. The TGA curve shows three weight losses as samples were thermally heated to 1000 °C. These weight losses appeared at the temperature intervals of 30–230 up 230–594 and 594–663 °C. The first weight loss is attributed to the removal of crystalline water which appears as from the surface of sample<sup>(11)</sup>.

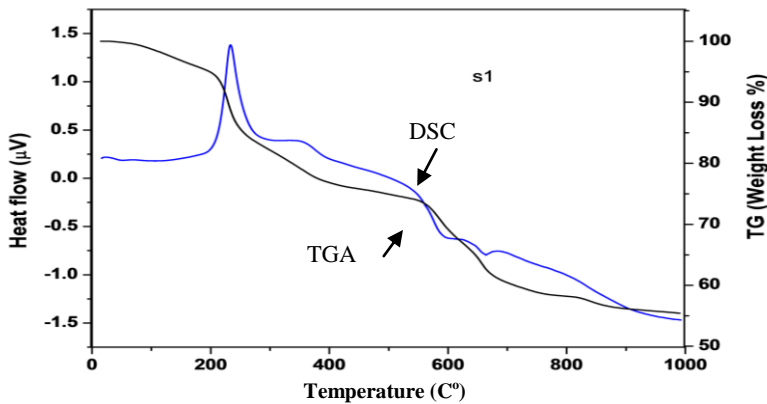


**Fig. 1.** TGA and DSC curves of the S1 gel powder after drying at 120° C for 2 days.

This is reflected in the DCS curves of S1 as the first strong exothermic peak centered at around 230°C, as shown in Fig.1. The second weight loss is illustrated in the endothermic peaks at 594 °C on the DSC curve of S1, which is most likely due to the elimination of the residual nitrates introduced in the preparation of the sol-gel<sup>(12)</sup>. The third weight loss shown by the TGA curve of S1 is due to crystallization temperature which supported by endothermic peak at 663 °C<sup>(13)</sup>. Therefore, the temperature of 500°C was chosen in present study for stabilization of the glass powder.

#### X-Ray diffraction analysis

Figure 2 illustrates the XRD patterns of S1, S2, S3, S4 and S5, where no discriminated peaks resulting from lattice periodicity are observed. This confirms that these samples are amorphous after heating at 500°C and characterized by the presence of broad diffraction peak (amorphous halo) in each glass samples analyzed<sup>(14,15)</sup>.

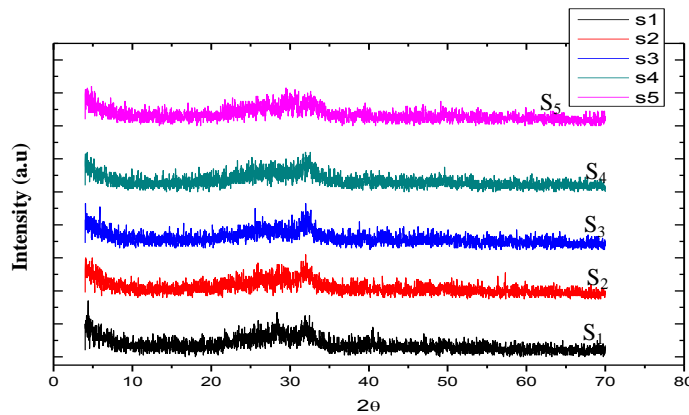


**Fig. 2.** XRD patterns of all gel glass samples after heat treatment at 500 °C before soaking in SBF.

*FTIR analysis for bioactive glass before soaking in simulated body fluid (SBF)*

The FTIR spectra of the bioactive glass before immersion in SBF are shown in Fig. 3. The main absorption bands for the amorphous sol-gel glass are observed at 1034, 948 and 786  $\text{cm}^{-1}$ . They are commonly attributed to asymmetric stretching vibration  $\text{Si-O-Si}$ <sup>(16)</sup> and  $\text{Si-O}$  stretching modes with non bridging oxygen<sup>(17)</sup> and  $\text{Si-O-Si}$  bridging silicon<sup>(18)</sup>, respectively.

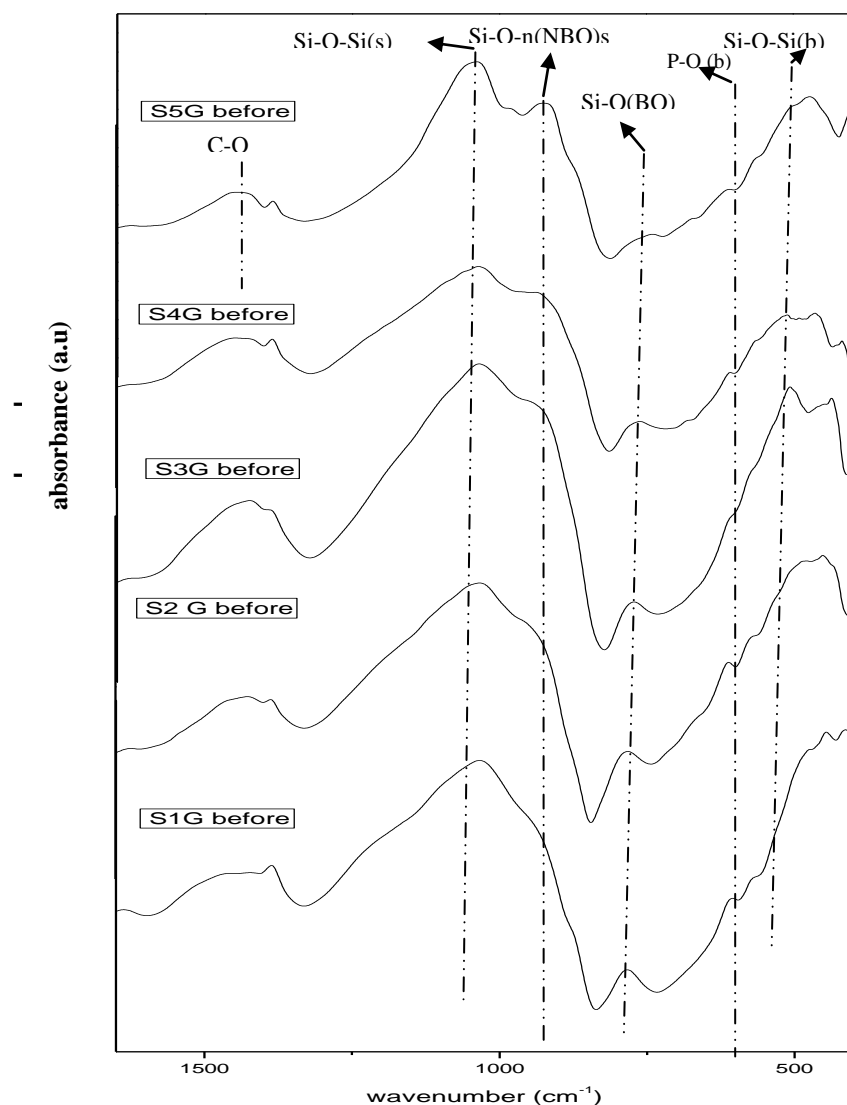


**Fig. 3.** FTIR spectra of all synthesized sol-gel samples with different concentrations of  $\text{Li}_2\text{O}$  before soaking in SBF.

These bands are generally observed in amorphous silica glasses for S1G before immersed in SBF as shown in Fig.3 .

A characteristic vibration bands at  $1476\text{ cm}^{-1}$ , which has been attributed to the C–O bending vibration from  $\text{CO}_3^{2-}$ <sup>(19)</sup>, was also observed with small amount in all samples of sol-gel glass. The symmetric bending mode of P–O (b) (amorphous calcium phosphate) at  $613\text{--}618\text{ cm}^{-1}$ <sup>(5)</sup> was appeared in all prepared bioactive glass.

Generally, the infrared spectra of poorly crystalline (amorphous) structure differ from those of well crystallized by several features such as broadening. This broadening was observed for the main absorption band (Si–O–Si) (s)<sup>(20)</sup>. Figure 3, shows the amorphous nature (disorder in the silicate and phosphate network) as found by Kansal *et al.*<sup>(21)</sup>. This was also noticed for all samples before soaking in SBF which was conformed to XRD.

In all of the spectra, an enhancement was observed in NBO in the range from 933 to about  $948\text{ cm}^{-1}$  and drop in Si–O–Si bridging in the range from 755 to about  $778\text{ cm}^{-1}$  with increment in lithium (modifier) and diminution of potassium (modifier). Thus, a little reduction in the molar concentration of glass network formers ( $\text{SiO}_2$  and  $\text{P}_2\text{O}_5$ ) occurred by this substitution, because of the lower atomic weight of Li compared to K. This indicates that the lithium is more effective as a modifier than potassium<sup>(10)</sup>.

#### *Characterization of bioactive glass after soaking in SBF*

##### *FTIR analysis*

The bioactive glass powder was immersed in SBF solution for 16 days and FTIR spectra were recorded for all prepared samples as shown in Fig.4. It can be noticed that, there are many variations in all samples after soaking in SBF for 16 days. These changes are in form of new absorption bands at around  $516\text{--}551\text{ cm}^{-1}$  for all glass samples which indicate to P–O bending (crystalline apatite) as found by Roman *et al.*<sup>(22)</sup>. Furthermore, new absorption bands located at  $1174\text{--}1181\text{ cm}^{-1}$  referring to presence of P=O stretching group as shown in Fig. 4. The last two bands can be used as an evidence for formation of the HCA layer at the surface of the bioactive glass<sup>(17)</sup>. All of the  $\text{Li}_2\text{O}$ -containing bioactive glass samples exhibit the formation of apatite layer after 16 days of soaking in SBF but with lesser amount. This is due to addition of Li to bioactive glass samples.

It can be seen that, the substitution of  $\text{K}_2\text{O}$  by  $\text{Li}_2\text{O}$  reduces the rate of glass dissolution and inhibits the formation of apatite due to improved chemical stability of glass<sup>(23)</sup>. The reason for this stability is electro negativity of  $\text{Li}^+$  which is higher than that of  $\text{K}^+$  in addition to ionic radius of  $\text{Li}^+$  which is lower than that of  $\text{K}^+$ , this result in more compacted glass network when  $\text{Li}_2\text{O}$  is substituted for  $\text{K}_2\text{O}$ <sup>(10)</sup>. This compactness of glass structure reduces the ion exchange resulting in reduction of silanol group Si–OH formation which is the nucleation site of apatite<sup>(24)</sup>.

This mechanism confirmed by reduction in the P-O bending band (crystalline apatite) and P=O stretching group with the enhancement of lithium content. Furthermore, the non-bridging oxygen Si-O-(n) NBO band in range ( $933\text{-}948\text{ cm}^{-1}$ ) contributes to the formation of silanol groups which is the nucleation site of hydroxyapatite and consequently controls the dissolution of network. This NBO group appeared clearly in glass samples S4 and S5 after soaking in SBF which indicates the cations not dissolved leads to reduction of apatite layer formation<sup>(25)</sup> in these samples as shown in Fig.4.

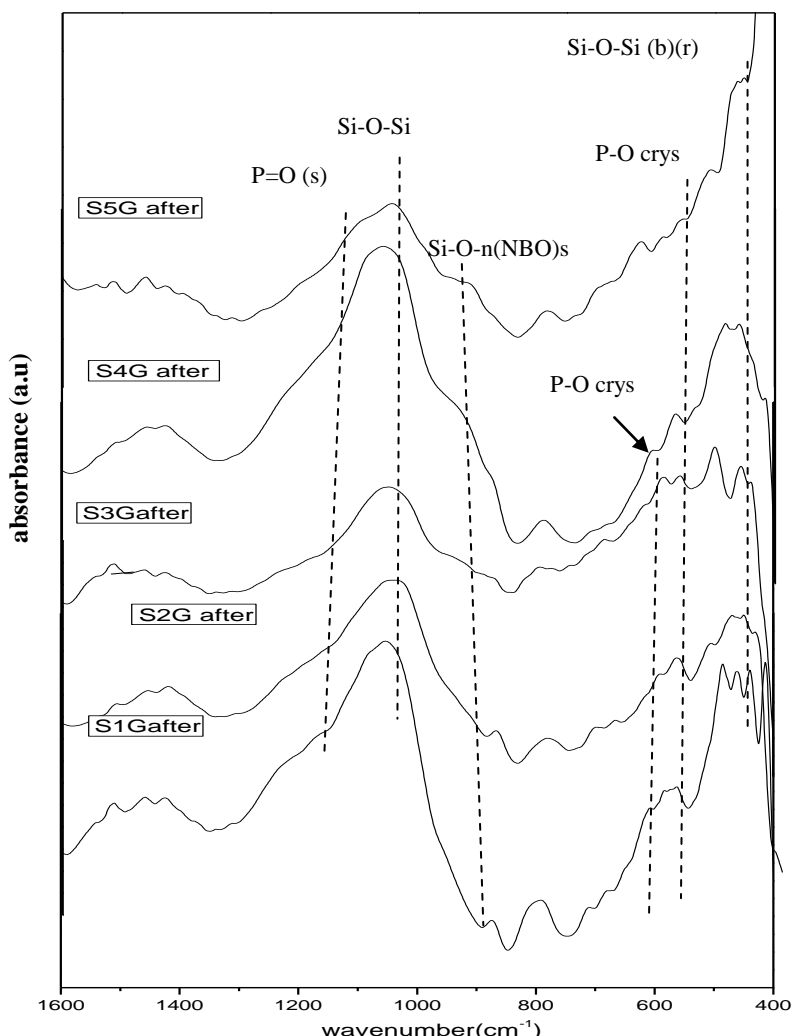


**Fig. 4.** FTIR spectra of all synthesized sol-gel glasses with different amounts of  $\text{Li}_2\text{O}$  after soaking in SBF.

*Results of inductive coupled plasma (ICP)*

A basic feature of bioactive materials is the formation of bonelike hydroxycarbonate apatite layer (HCap) on their surface *in-vitro* when the temperature, pH and ionic composition of the fluid are nearly equal to that of blood plasma<sup>(26)</sup>. Changes in SBF composition after soaking of bioactive glass samples during a period 16 days are shown in Fig. 5 and 6.

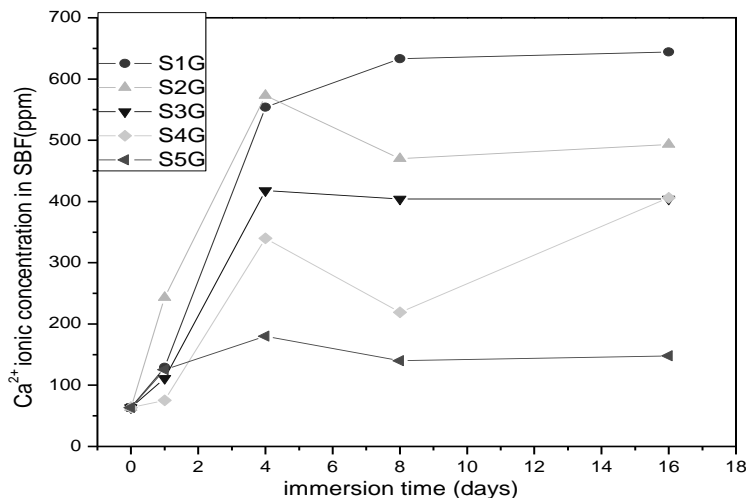


**Fig. 5.** Calcium ion concentration of SBF solution after immersion of bioactive glass samples for various periods.

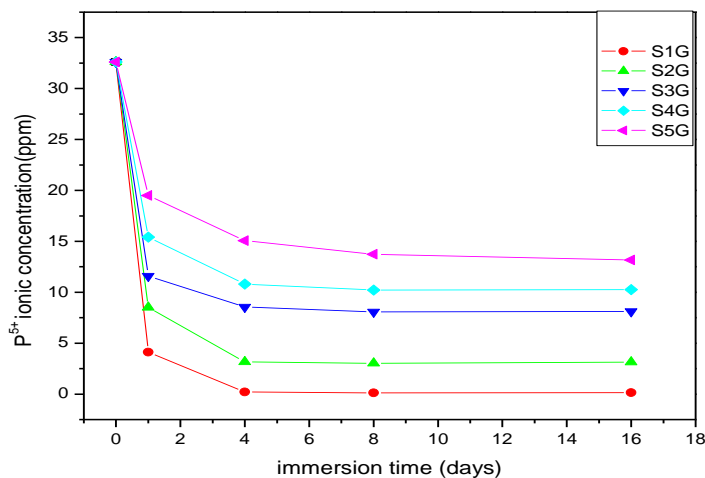


**Fig. 6.** Phosphorus ion concentration of SBF solution after immersion of bioactive glass for various periods.

As can be seen, Ca ion concentration of SBF increased from 63 to 644 ppm for S1 glass sample up to the end of evaluating period. In S2,S3,S4 and S5 glass samples , the Ca<sup>2+</sup> concentrations changed, reaching 473, 418, 340 and 180 ppm, respectively on 4<sup>th</sup> day. On 8<sup>th</sup> day, the Ca<sup>2+</sup> concentration decreased in S2,S3,S4 and S5 glass samples while it return to enlarge reaching to 393, 404, 406 and 148 ppm, respectively on 16<sup>th</sup> day, as shown in Fig. 5.

On the other hand, the P<sup>5+</sup> concentration decreased gradually from 32.6 ppm reached to 0.126, 0.023, 0.071, 0.207 and 0.164 ppm for S1, S2, S3, S4 and S5 bioactive glass samples, respectively during the first 8 days immersion in SBF, as shown in Fig. 6.

Therefore, Ca<sup>2+</sup> increases during the first 8 days as compared to initial Ca<sup>2+</sup> of the solution which is due to Ca<sup>2+</sup> ions exchange with H<sup>+</sup> or H<sub>3</sub>O<sup>+</sup> ions into in the SBF solution . It follows that Ca<sup>2+</sup> ions concentration decreases gradually<sup>(27)</sup>. At the same time, for all the glass samples, the P<sup>5+</sup> concentration decreases gradually to reach lower value after 16 days which is due to P<sup>5+</sup> ions which leave SBF to be deposited on the surface of samples. From the Ca<sup>2+</sup> and P<sup>5+</sup> concentration variations mentioned, it can be stated that the Ca<sup>2+</sup> and P<sup>5+</sup> decreases due to formation of calcium phosphate apatite layer which is balanced by the solution exchange<sup>(28)</sup>.

On the other hand, the Ca<sup>2+</sup> ions in SBF solutions increase with enhancement of Li<sub>2</sub>O content in bioactive glass samples. But the behavior of lower Ca<sup>2+</sup> concentration region is varying from sample to another depending on the Li<sub>2</sub>O content and it is illustrated in Fig. 5. According to previous investigation by some authors as Ma *et al.*<sup>(29)</sup> and Diba *et al.*<sup>(30)</sup>, they found that K<sub>2</sub>O and Li<sub>2</sub>O are thought to behave as a network modifiers, and could enter into glass structure and induce the formation of NBOs.

Based on the ICP results, the enlargement of calcium and phosphorus ion concentrations together with enhancement of lithium content is attributed to the lower ionic radius of lithium comparing to potassium which results in increase of network strength<sup>(31)</sup>. This principle attributes to the process of dissolution to overcome the precipitation and therefore decreases the formation of hydroxyapatite layer on glass samples when increasing lithium ion content.

#### *Investigations of scanning electron microscope and dispersive X-ray spectrometer*

Scanning electron microscopy (SEM) provides high resolution in combination with good depth of field and with an energy dispersive X-ray spectrometer (EDX) attached which identifies chemical composition within the microstructure at one location simultaneously<sup>(32)</sup> .

The SEM images of glass before soaking as shown in Fig.7 is characterized by a nearly smooth surface formed on glass pellet. The growth of white particles can be observed on its surface when soaking in SBF for 16 day is represented in Fig. 7 and 8. Thus, glass surface becomes covered with a layer of spherical forms

of apatite with dimensions of nearly from 0.86 to 1.7 $\mu$ m. An obvious difference in the surface morphology of all bioactive glass samples is observed after immersion in SBF, indicating the formation of apatite layer on the surface with different amounts. Also, the morphological structure of apatite-like layer varies with the lithium oxide content of glasses. An obvious difference in the surface morphology of all bioactive glass samples is observed after immersion in SBF, indicating the formation of apatite layer on the surface with different amount. Also, the morphological structure of apatite-like layer varies with the lithium oxide content of glasses.

A thick layer of apatite is noticed on the surface of S1G glass samples in Fig.7 when compared to other Li<sub>2</sub>O substituted glass samples as shown in Fig. 8. On surfaces of samples S1, S3 and S5, crystalline aggregates are observed, but the size and the relief of the crystalline particles decreases with the enhancement of Lithium content . Further evidence to confirm the presence of apatite layers on the surfaces of glass samples with different magnitudes, was assured using the EDX technique before and after the soaking in the SBF.

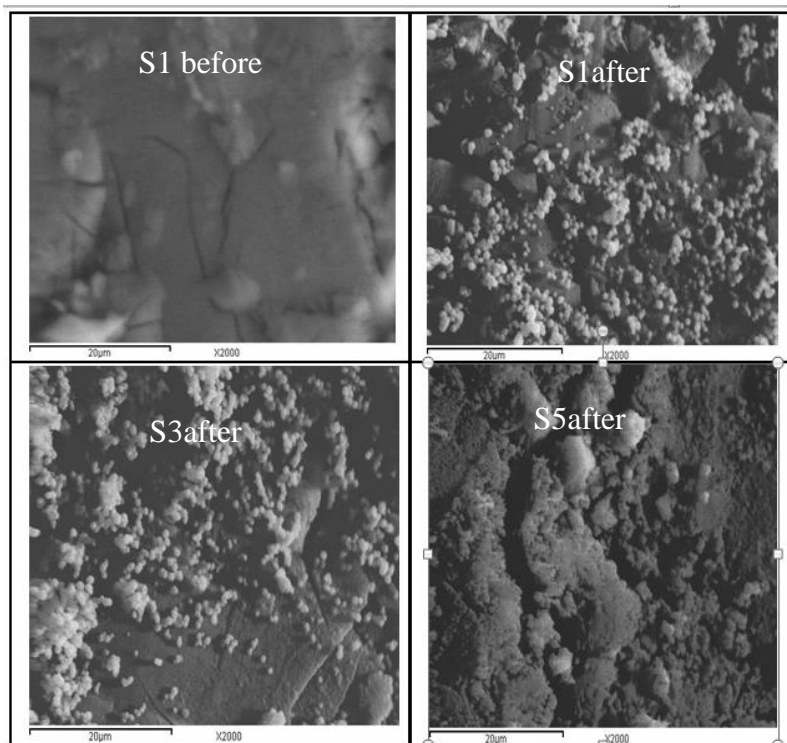


**Fig. 7.** SEM images x2000 of bioactive glass sample S1 before and S1, S3 and S5 after soaking in SBF for 16 days .

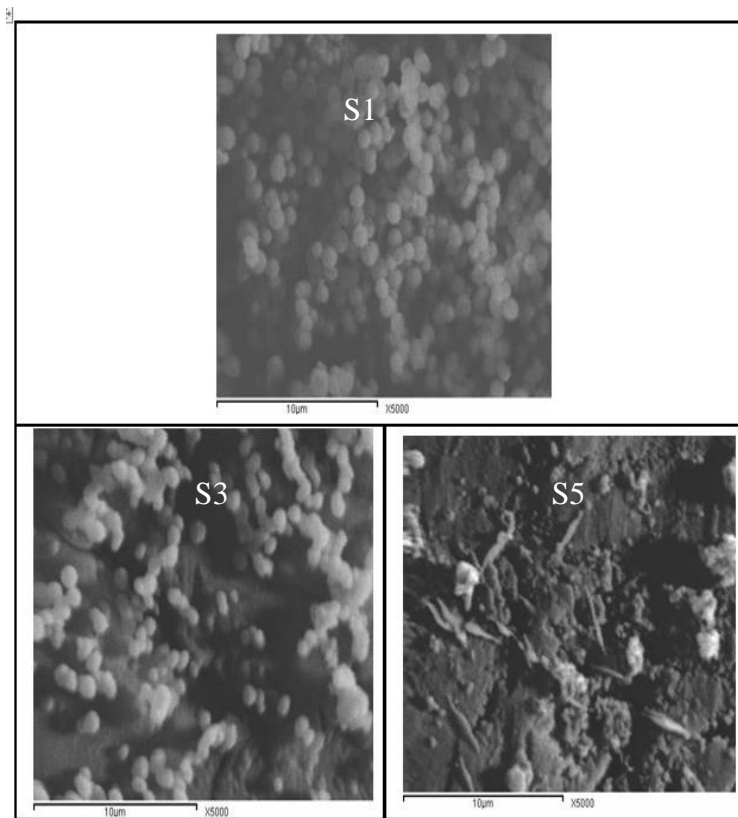


**Fig. 8.** SEM images x5000 of bioactive glass sample S1, S3 and S5 samples after soaking in SBF solution for 16 days.

Figure 9 shows the EDX trace from the surface of glass S1G sample before soaking in the SBF indicating the presence of Ca, Cl, K, O, Si and P. EDX spectrum from the same sample S1G after soaking in SBF for 16 days revealed that increase of significant peaks for Ca and P elements and diminution of peak for Si element. Furthermore, new peak for carbon (C) is observed after soaking in SBF as found by Hong *et al.*<sup>(33)</sup>. This indicates the precipitation of the carbonated apatite layer on the glass surface. These precipitates are believed to be formed through the dissolution and re-precipitation process during the soaking time. Also, carbonated apatite layer is rich with Ca and P is detected by XRD and FTIR analyses, these findings are in accordance with results obtained by Bretcanu *et al.*<sup>(34)</sup>.

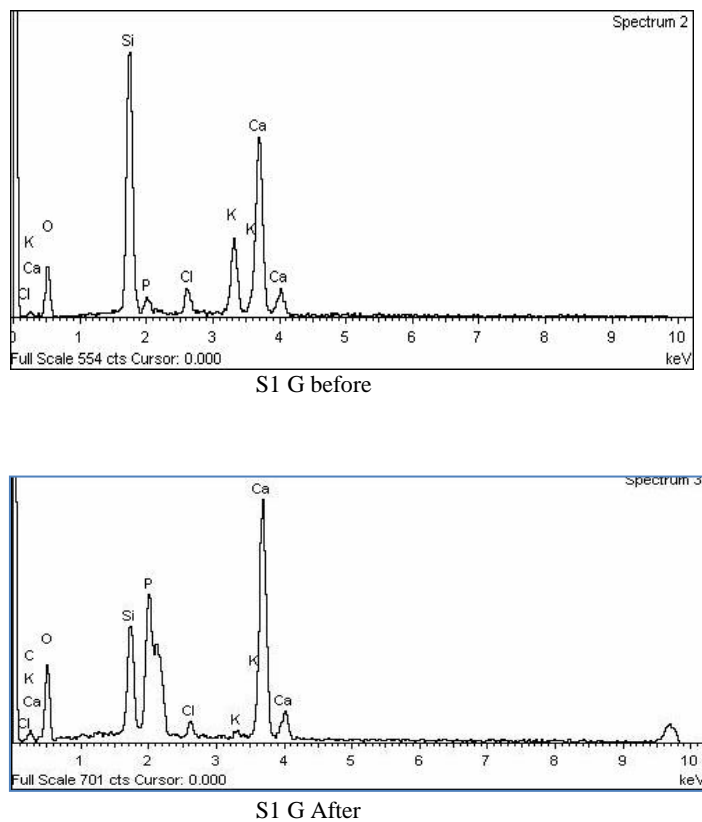


**Fig. 9. EDX spectra of S1 sample before and after soaking in SBF for 16 days.**

### Conclusion

- According to the thermal analysis (DSC and TGA) investigations, the results allowed us to raise the temperature at 500°C to reach stabilization of glass powder.
- XRD pattern showed that all prepared glass at 500°C is completely amorphous in nature, characterized by absence of diffraction peaks .
- FTIR spectroscopy applied after immersion in the simulated body fluid (SBF) and indicated that Li<sub>2</sub>O suppress the crystal growth of the apatite on the surface of the glass samples.
- The elemental analysis demonstrated that, the decrease in the phosphorus and calcium concentration in SBF was attributed to formation of (bone-like) apatite layer on the surface of the prepared samples by consumption of the calcium and phosphate ion from the SBF solution.

- SEM and EDX techniques illustrated that glass surface becomes covered with a layer of spherical forms of apatite with dimensions of about 0.86-1.7µm.
- The apatite layer formation depends on the concentration of Li<sub>2</sub>O which represents decrement *in vitro* bioactivity of glass.
- When partial substitution of Li<sub>2</sub>O for K<sub>2</sub>O was carried out in glass composition, the crystallinity of the grown layer was decreased and the formation of apatite-like layer is delayed, confirming that, not all glass and glass-ceramic surfaces are equally active for nucleation of apatite crystals.
- The formation of apatite layer depends on the concentration of Li<sub>2</sub>O. Also, it is possible to develop bioactive glass system by percentage of lithium content which controls the dissolution rate of this system to be applied *in vivo* for dentine and bone replacement.

#### References

1. **Fathi, M.H. and Doostmohammadi, A.**, Bioactive glass nanopowder and bioglass coating for biocompatibility improvement of metallic implant. *J. Mater. Process. Technol.* **209**, 1385–1391 (2009).
2. **Hench, L.L.**, Bioactive glasses and glass-ceramics, *Bioceramics, Mater. Sci. Forum*, **293**, 37–64 (1999).
3. **Mabrouk, M., Mostafa, A.A., Oudadesse, H., Mahmoud, A.A., Gaafar, A.M. and El-Gohary, M.I.**, Fabrication, characterization and drug release of ciprofloxacin loaded porous polyvinyl alcohol/bioactive glass scaffold for controlled drug delivery. *Bioceram Dev. Appl.* ISSN: 2090-5025 BDA (2013).
4. **Mezahi, F.Z., Lucas-Girot, A., Oudadesse, H. and Harabi A.**, Reactivity kinetics of 52S4 glass in the quaternary system SiO<sub>2</sub>-CaO-Na<sub>2</sub>O-P<sub>2</sub>O<sub>5</sub>: influence of the synthesis process: Melting versus sol-gel. *Journal of Non-Crystalline Solids*, **361**, 111-118 (2013).
5. **Saravanapavan, P., Jones, J.R., Pryce, R.S. and Hench, L.L.**, Bioactivity of gel-glass powders in the CaO-SiO<sub>2</sub> system: A comparison with ternary (CaO-P<sub>2</sub>O<sub>5</sub>-SiO<sub>2</sub>) and quaternary glasses (SiO<sub>2</sub>-CaO-P<sub>2</sub>O<sub>5</sub>-Na<sub>2</sub>O). *J. Biomed. Mater. Res.* **66 A**, 110–119 (2003).
6. **Kokubo, T., Kushitani, H., Sakka, S., Kitsugi, T. and Yamamuro, T.**, Solutions able to reproduce *in vivo* surface-structure changes in bioactive glass-ceramic A-W. *J. Biomed. Mater. Res.* **24**, 721-34 (1990).
7. **Pietak, M., Reid, J.W., Stott, M.J. and Sayer, M.**, Silicon substitution in the calcium phosphate bioceramics. *Biomaterials*, **28**, 4023-32 (2007).
8. **Clement-Lacroix, P., Morvan, F., Roman-Roman, S., Vayssiere, B. and Belleville, C.**, Lrp5- independent activation of Wnt signaling by lithium chloride increases bone formation and bone mass in mice. *Proc.Natl. Acad. Sci.* **102**, 17406–17411(2005).

9. **Zamani, A., Omrani, R.G., Nasab, Masoud Mousavi**, Lithium's effect on bone mineral density. *Bone*, **44**, 331–334 (2009).
10. **Khorami, M. , Hesaraki , S., Behnamghader , A., Nazarian , H., Shahrabi, Sara**, *In vitro* bioactivity and biocompatibility of lithium substituted 45S5 bioglass. *Materials Science and Engineering C*, **31**, 1584–1592 (2011).
11. **Tiznado-Orozco, Gaby E., Garc'ia-Garc'ia, R. and Reyes-Gasga, J.**, Structural and thermal behaviour of carious and sound powders of human tooth enamel and dentine. *J. Phys. D: Appl. Phys.* **42**, 8 (2009).
12. **El Gohary, M.I., Tohamy, K.M., El-Okr, M.M., Ali, A.F. and Soliman, I.E.**, Influence of composition on the *in-vitro* bioactivity of bioglass prepared by a quick alkali-mediated sol-gel method. *Nat. Sci.* **11**, 26-33 (2013).
13. **Ganesan, M. , Dhananjeyan, M.V.T., Sarangapani, K.B. and Renganathan , N.G.**, Lithium ion conduction in sol-gel derived lithium samarium silicate solid electrolyte. *Journal of Alloys and Compounds* , **450** , 452–456 (2008).
14. **Li, N., Jie, Qing, Sumin, Zhu and Wang, Ruoding**, A new route to prepare macroporous bioactive sol-gel glasses with high mechanical strength, *Materials Letters*, **58**, 2747– 2750 (2004).
15. **Balamurugan, A., Balossier, G., Michel J., Kannan, S., Benhayoune, H., Rebelo, A. H. S. and Ferreira, J. M. F.**, Sol gel derived SiO<sub>2</sub>-CaO-MgO-P<sub>2</sub>O<sub>5</sub> bioglass system—preparation and *in vitro* characterization. *J. Biomed. Mater. Res. Part B: Appl. Biomater.* **83**, 546-553 (2007).
16. **Merzbacher, C.I. and White, W. B.**, The structure of alkaline earth aluminosilicate glasses as determined by vibrational spectroscopy. *Journal of Non-Crystalline Solids*, **130**, 18-34. (1991).
17. **Shi, J., Natália, M. Alves and João, F. Mano**, Thermally Responsive Biominerization on Biodegradable Substrates, *Adv. Funct. Mater.* **17**, 3312–3318 (2007).
18. **Palusziewicz, C., Blaz' ewicz, M., Podporska, J. and Gumula, T.**, Nucleation of hydroxyapatite layer on wollastonite material surface: FTIR studies. *Vibrational Spectroscopy*, **48**, 263–268 (2008).
19. **EIBatal, Fatma H., Abooz, M.A. and Hamdy, Y.M.**, Preparation and characterization of some multicomponent silicate glasses and their glass-ceramics derivatives for dental applications. *Ceramics International*, **35**, 1211–1218 (2009).
20. **Rey, C., Combes, C., Drouet, C., Lebugle, A., Sfih, H. and Barroug, A.**, Nanocrystalline apatites in biological systems: characterization, structure and properties. *Mat.-wiss. u. werkstofftech*, **38**, 996-1002 (2007).
21. **Kansal, I., Dilshat, U., Tulyaganov, Ashutosh Goel, Pascual, Maria J. and Ferreira, Jose M.F.**, Structural analysis and thermal behavior of diopside-fluorapatite-wollastonite-based glasses and glass-ceramic. *Acta Biomaterialia*, **6**, 4380-4388 (2010).

22. **Román, J., Padilla, S. and Vallet-Regí, M.**, Sol-gel glasses as precursors of bioactive glass-ceramics. *Chem. Mater.* **15**, 798–806 (2003).
- 23 **Wallace, K.E., Hill, R.G., Pembroke, J.T., Brown, C.J. and Hatton, P.V.**, Influence of sodium oxide content on bioactive glass properties, *J. Materials Science: Materials in Medicine*, **10**, 697–701 (1999).
24. **Ohtsuki, C., Kushitani, H., Kokubo, T., Kotani, S. and Yamamuro, T.**, Apatite formation on the surface of ceravital-type glass-ceramic in the body. *J. Biomed. Mater. Res.* **25**, 1363–1370 (1991).
25. **Oréfice, R.L., Henchband, L.L. and Brennan, A. B.**, In vitro bioactivity of polymer matrices reinforced with a bioactive glass phase, **11**, 78–85 (2000).
26. **Muhammad, U.H., Saqlain, A. S., Shah, Z. A. and Ahmad, S.**, Dissolution behavior of bioactive glass ceramics with different CaO/MgO ratios, *Ceramics – Silikáty*, **54**, 8–13 (2010).
27. **Izquierdo-Barba, I., Salinas, A. J. and Vallet-Regí, M.**, Effect of the continuous solution exchange on the in vitro reactivity of a CaO-SiO<sub>2</sub> sol-gel glass. *Journal of Biomedical Materials Research*, **51**, 191–199 (2000).
28. **Debdas, R.**, In vitro reactivity of Na<sub>2</sub>O–MgO–SiO<sub>2</sub> glasses. *Journal of Physics and Chemistry of Solids*, **68**, 2321–2325 (2007).
29. **Ma, J., Chen , C.Z., Wang , D.G. and Hu, J.H.**, Synthesis, characterization and in vitro bioactivity of magnesium-doped sol–gel glass and glass-ceramics. *Ceramics International*, **37**, 1637–1644 (2011).
30. **Diba, M., Tapia, F. and Boccaccini, A.R.**, Magnesium-containing bioactive glasses for biomedical applications. *international Journal of Applied Glass Science*, **3**, 221–253 (2012).
31. **Oliveira, J.M., Correia, R.N., Fernandes, M.H.**, Effects of Si speciation on the in vitro bioactivity of glasses. *Biomaterials*, **23**, 371–379 (2002).
32. **Kokubo, T.**, “*Bioceramics and Their Clinical Applications*”, Woodhead Publishing Limited and CRC Press LLC , Cambridge, England, 174–760 (2008).
33. **Hong, Z., Liu, A., Chen, Li , Chen, X. and Jing, X.**, Preparation of bioactive glass ceramic nanoparticles by combination of sol–gel and coprecipitation method. *J. Non-Crystalline Solids*, **355**, 368–372 (2009).
34. **Bretcanu, O., Spriano, S., Vitale, C.B. and Vern 'E.**, Synthesis and characterization of co-precipitation-derived ferrimagnetic glass-ceramic. *J. Mater. Sci.*, **411**, 1029–1037 (2006).

(Received 10/2/2014;  
accepted 25/3/2014)

## دراسة تأثير الليثيوم على تكون طبقة الأباتيت على سطح الزجاج فى النظام $\text{SiO}_2\text{-P}_2\text{O}_5\text{-CaO-K}_2\text{O}$

محمد إسماعيل الجوهرى، صفاء محمد محي الدين<sup>\*</sup>، سحر محمد عوض<sup>\*</sup>،  
أسماء محمد التهامى<sup>\*</sup> و اسلام سليمان  
قسم الفيزياء – شعبة الفيزياء الحيوية – كلية العلوم بنين و<sup>\*</sup>قسم الفيزياء – شعبة  
الفيزياء الحيوية – كلية العلوم بنات – جامعة الازهر – مدينة نصر- القاهرة –  
مصر.

تم فى هذه الدراسه الحاليه تحضير الزجاج بطريقة السول الجيل فى النظام  $\text{SiO}_2\text{-P}_2\text{O}_5\text{-CaO-K}_2\text{O}$ . وقد تم فحص تأثير هذا الإبدال على قدرة النظام على تكون طبقة الأباتيت خارج جسم الإنسان (*in vitro*) وكذلك على التغيرات فى بناء النظام الزجاجي. ثم تم دراسة السلوك الحراري للعينات المحضرة عن طريق الماسح الحراري التقاضلى (DSC) ومنحنى التحليل الثنائى الحراري (TGA). تم استخدام تحليل حيد الأشعه السينيه (XRD) للتعرف على الأطوار البلوريه التي تم ترسيبها فى العينات قبل أن تغمر فىسائل المحاكى لبلازما دم الإنسان. تم ايضا قياس (FTIR) لعينات الزجاج قبل وبعد الغمر فىسائل المحاكى لبلازما دم الإنسان. نتائج النشاط الحيوى لهذه الدراسه توضح تكوين طبقة الأباتيت والذى تعتمد على تركيزات الليثيوم واضافته يمثل نقص فى النشاط الحيوى للزجاج داخل جسم الإنسان (*in vivo*). وقد بينت النتائج أيضا أنه من الممكن تحضير زجاج نشط حيويا بواسطة التحكم فى تركيز الليثيوم الذى يتحكم فى معدل النوبان للاستخدام فى تطبيقات الاسنان والعظم داخل جسم الإنسان (*in vivo*).